Respiratory Physiology & Neurobiology 293 (2021) 103722

Contents lists available at ScienceDirect

Respiratory Physiology & Neurobiology

journal homepage: www.elsevier.com/locate/resphysiol

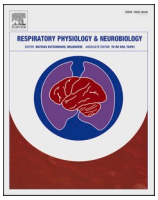

Lung inflammation and simulated airway resistance in infants with cystic fibrosis

Emily M. DeBoer [a,b,*], Julia S. Kimbell [c], Kaci Pickett [d], Joseph E. Hatch [c], Kathryn Akers [e], John Brinton [b,d], Graham L. Hall [f,g], Louise King [h], Fiona Ramanauskas [h], Tim Rosenow [f], Stephen M. Stick [f], Harm A. Tiddens [i], Thomas W. Ferkol [e], Sarath C. Ranganathan [h], Stephanie D. Davis [c], AREST CF

[a] University of Colorado Anschutz Medical Campus, Aurora, CO, United States
[b] Breathing Institute at Children's Hospital Colorado, Aurora, CO, United States
[c] University of North Carolina School of Medicine, Chapel Hill, NC, United States
[d] Colorado School of Public Health, Aurora, CO, United States
[e] Washington University School of Medicine, St. Louis, MO, United States
[f] Telethon Kids Institute and Perth Children's Hospital, U. of Western Australia, Perth, WA, Australia
[g] School of Physiotherapy and Exercise Science, Curtin University, Perth, WA, Australia
[h] Royal Children's Hospital and Murdoch Children's Research Institute, U. of Melbourne, Parkville, VIC, Australia
[i] Erasmus MC and Sophia Children's Hospital, Rotterdam, the Netherlands

ARTICLE INFO

Edited by Mathias Dutschmann

Keywords:
Pediatrics
Airway mechanics
Computational fluid dynamics

ABSTRACT

Cystic fibrosis (CF) is characterized by small airway disease; but central airways may also be affected. We hypothesized that airway resistance estimated from computational fluid dynamic (CFD) methodology in infants with CF was higher than controls and that early airway inflammation in infants with CF is associated with airway resistance. Central airway models with a median of 51 bronchial outlets per model (interquartile range 46,56) were created from chest computed tomography scans of 18 infants with CF and 7 controls. Steady state airflow into the trachea was simulated to estimate central airway resistance in each model. Airway resistance was increased in the full airway models of infants with CF versus controls and in models trimmed to 33 bronchi. Airway resistance was associated with markers of inflammation in bronchoalveolar lavage fluid obtained approximately 8 months earlier but not with markers obtained at the same time. In conclusion, airway resistance estimated by CFD modeling is increased in infants with CF compared to controls and may be related to early airway inflammation.

1. Introduction

Cystic fibrosis (CF) is an autosomal recessive genetic disease marked by abnormal mucus production, chronic airway inflammation and infection leading to structural airway injury and bronchiectasis (O'Sullivan and Freedman, 2009; Sanders et al., 2014). Human and animal studies have demonstrated that the CF airway is abnormal from birth, with airway shape abnormalities, including reduced caliber and less circular shape, seen in the CF human infant and CF pig at birth (Meyerholz et al., 2018, 2010; Ranganathan et al., 2017). Despite these congenital abnormalities, airway disease in infants with CF is often clinically "silent" without overt respiratory symptoms. Cohort studies have been conducted during infancy and young childhood to identify this subtle, early airway disease (Ranganathan et al., 2017; Simpson et al., 2013; Sly et al., 2013). To better understand this airway disease, evaluations beyond history and physical examination are performed, including chest computed tomography (CT) scans, multiple breath washout, infant pulmonary function tests, and bronchoscopy with bronchoalveolar lavage fluid (BALF) collection (Ramsey et al., 2016). Imaging studies have confirmed abnormal airway findings including abnormal tracheal cartilage, tracheomalacia, and bronchiectasis (Fischer et al., 2014; Meyerholz et al., 2010; Rosenow et al., 2015).

Chest CT images are the gold standard to define airway structure. Computational fluid dynamic (CFD) modeling methods can be used to

* Corresponding author at: Children's Hospital Colorado, 13123 E 16thAve. B-395, Aurora, CO, 80045, United States.
E-mail address: Emily.deboer@childrenscolorado.org (E.M. DeBoer).

https://doi.org/10.1016/j.resp.2021.103722
Received 28 January 2021; Received in revised form 17 May 2021; Accepted 17 June 2021
Available online 19 June 2021

estimate functional abnormalities from volumetric chest CT images. The primary results of CFD modeling are estimated airway pressures, airway resistance, and airflow patterns. CFD techniques have been used to reveal increased airway resistance in infants with left pulmonary artery sling (Qi et al., 2014) and in infants with tracheomalacia (Gunatilaka et al., 2020), and decreases in resistance have been noted after airway stenting (Ho et al., 2012). Based on CFD model simulations of the CF pig airway, the tracheal shape differences seen at birth result in both increased airway resistance and airflow velocity (Awadalla et al., 2014). CFD models have also predicted alterations in drug particle deposition in the pig model and older patients with CF (Bos et al., 2015). CFD has not been described in infants with CF during the clinically silent period.

We hypothesized that airway resistance, estimated using CFD models created from chest CT scans, would be higher in infants with CF than controls. We explored CFD models using all visualized airways and a model that isolated more central airways by trimming the most distal airways. A secondary aim was to evaluate the association of early airway inflammation with airway resistance in infants with CF.

2. Methods

2.1. Study subjects

This project utilized volumetric chest CT images and physiologic results from 20 infants who participated in an international prospective observational study entitled the Viral Pathogenesis of Early Cystic Fibrosis Lung disease (NCT01973192)(Deschamp et al., 2019). Data from two study sites: 1) Royal Children's Hospital in Melbourne, AUS and 2) Riley Children's Hospital in Indianapolis, Indiana, USA are presented in this manuscript. CT scans from two children with CF had poor image quality and were excluded a priori from this analysis. Control subjects were infants with leukemia who had volumetric chest CT imaging between 10 and 16 months of age and who had no "significant lung disease" as determined by the investigators. Control children were enrolled in a separate research study at Royal Children's Hospital in Melbourne and underwent the same research CT scan protocol as CF study subjects. Study protocols were approved by the institutional review boards at all enrolling sites and written consent was obtained from the parents or caregivers.

2.2. Study design

Bronchoscopy and BALF collection as well as infant lung function tests were conducted twice in the infants with CF: at study enrollment (Visit 1) and approximately eight months later (Visit 2) as previously described (Deschamp et al., 2019; Pittman et al., 2017). The infant lung function outcomes were forced expiratory volume at 0.5 s (FEV 0.5) and forced expiratory flow at 75 % of forced vital capacity (FEF75). These infant lung function parameters were reported based on Z-scores. When performing the bronchoscopy, a total of four 1 mL/kg aliquots of sterile normal saline were instilled into subsegmental bronchi of the right middle lobe and lingula. The collected lavage fluid was pooled, with an aliquot sent to the clinical microbiology and cytology laboratories at each site for bacterial culture and cell counts. The main outcome of inflammation was percent of the nucleated cells that were neutrophils (%neutrophils). The remaining lavage fluid was pelleted at 900 g for 10 min and the supernatant was frozen at -80C and sent to Washington University in St. Louis for interleukin 8 (IL8) analysis using commercially available sandwich enzyme immunoassays (R&D Systems, Minneapolis, MN; USA). The urea dilution method was used to determine cell counts and cytokine concentrations in the epithelial lining fluid (Rennard et al., 1986).

2.2.1. Chest CT acquisition and scoring

A chest CT scan was obtained during Visit 2. Control children were imaged for clinical evaluation of metastases and measurements were collected at one study visit. The chest CT without contrast was used for the CFD. All children had general anesthesia according to local site protocols in the supine position. Standardized recruitment maneuvers consisting of 10 consecutive slow breaths up to a set lung capacity (37−40 cm H_2O) with a positive end-expiratory pressure of 5 cm H_2O were administered to avoid atelectasis. Pressure was held steady at 25 cm H_2O during an inspiratory volumetric scan with these parameters: 400 msec rotation time, 80−120 kV, 80 mAs, pitch 1.2, 0.63 collimation, 1.0 mm slice thickness or less, and high spatial reconstruction. Chest CTs were scored by a single reader using the Perth Rotterdam Annotated Grid Morphometric Analysis (PRAGMA-CF) methodology for bronchiectasis and %Airway Disease (Rosenow et al., 2015).

2.2.2. Airway modeling and CFD

CFD methodology was adapted from previous upper airway applications (Frank-Ito et al., 2019; Kimbell et al., 2013), assuming constant inspiratory velocity across the tracheal inlet. Briefly, three-dimensional (3D) reconstructions of the conducting airways were segmented and measured using semi-automated Mimics Pulmonary module (Reynisson et al., 2015) (Mimics™ v.18, Materialise, Inc., Plymouth, MI; USA) (Fig. 1a). This module uses dynamic region growing to find connected airways, with region-of-interest erosion and dilation to eliminate segmentation leakage into the adjacent lung. Endotracheal tubes were subtracted from the segmentations, and the airway models were filled and smoothed to create an intact trachea and finalize airway lumen boundaries (Fig. 1b). Cross-sectional area and circumference of the distal trachea, below the distal end of the endotracheal tube and just proximal to the transition of the carina, and the mainstem bronchi at their midpoints, were obtained perpendicular to the airway centerline (Fig. 1c). Airway geometry was converted to stereolithography (STL) format, and computer-aided design software (ICEM-CFD™, ANSYS, Inc, Lebanon, NH; USA) was used to cut the tracheal inlet and the distal outlets. Outlets were cut by planes placed perpendicular to each airway centerline (Fig. 1c) just proximal to the tapering of each airway end. ICEM-CFD was also used to generate 3D graded tetrahedral meshes with approximately 4 million elements (Fig. 2a,b). A mesh refinement study using meshes with 1–8 million elements indicated that airway resistance varied by less than 0.7 % with refinement beyond 4 million cells.

In an attempt to further standardize the models, the maximum number of outlets that were present on a subset of 15 models (all 7 controls, 8 randomly selected CF) was counted and these 15 models were trimmed to have the same number of outlets in each lobe. To control for size differences, these trimmed models were scaled to the average tracheal cross-section of the controls. Graded tetrahedral meshes were also created from the trimmed models and the trimmed-and-scaled models.

A steady inspiratory flow of 5,644.9 mL/min (twice the minute volume (Kimbell et al., 2001)) was applied to the trachea of all models based on body weight of the first five infants included in the control cohort (11.27 ± 1.81 kg) and minute ventilation estimates of infants described by Nguyen and colleagues (Nguyen et al., 2013) and was simulated using commercial CFD software (Fluent™v. 14.5, ANSYS Inc. Lebanon, NH; USA) (Fig. 2c) (Wofford et al., 2015). Airway resistance (the primary outcome) was calculated as $\Delta p/Q$, where Δp is pressure difference in Pascals between proximal and distal airways and Q is the flow in milliliters per second (Fig. 2c). Airway pressure at the distal airway outlets was set to zero (Fig. 2c). A tracheal plane parallel to the inlet plane was created at the site of the measurement of tracheal cross-sectional area and tracheal resistance (proximal to the tracheal plane) and bronchial resistance (distal to the tracheal plane) were calculated (Fig. 2b). Reynolds numbers were calculated at the tracheal plane to assess flow structure. A Reynolds number <2700 was considered appropriate for modeling flow as laminar (Ben-Dov and Cohen, 2007; Hof et al., 2003). All models had Reynolds numbers <1100, therefore laminar methods were used for simulations.

Figures visualizing CFD outputs were made using Fieldview™

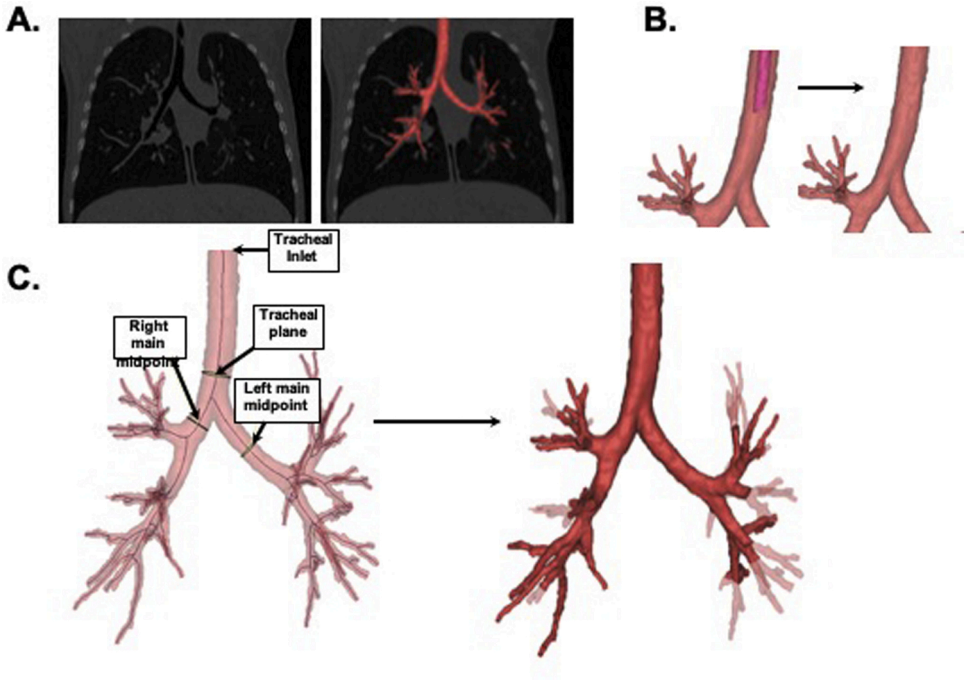

Fig. 1. Airway Segmentation. (A) Airway segmentation overlaid on axial chest CT image. (B) Example of filled-in trachea (subtraction of endotracheal tube). (C) Airway centerline with tracheal and bronchial cross-sectional area measurements. Subset model (dark red) shows distal airways trimmed to 33 outlets.

(Intelligent Light, Lyndhurst, NJ; USA) and Fluent™v. 14.5 (ANSYS Inc. Lebanon, NH; USA) (Fig. 2c).

2.2.3. Validation with lobar analysis

Two chest CT scans had full volumetric expiratory scans obtained as part of an additional protocol. The proportion of ventilation to each lobe was calculated and compared to CFD estimates of lobar flow (Supplement Fig. 1).

2.2.4. Outcomes

Airway resistance was estimated for the full airway model in both CF (N = 18) and control (N = 7) groups. This outcome is referred to as Airway resistance (Raw). Tracheal resistance was estimated for the trachea (between the inlet and the tracheal plane), and bronchial resistance was estimated distal to the tracheal plane (Fig. 2b). A subset of patients (all 7 control, 8 randomly selected CF) also had resistance estimated in models trimmed to 33 outlets and in trimmed models with the inlet size scaled.

2.3. Analysis

Patient demographic and clinical measures are summarized by group. Exact Wilcoxon Rank Tests compared resistance between CF and control groups due to the small sample size. Fisher's Exact test compared categorical variables between groups. Results are presented as a median [interquartile-range] with a p-value. Linear regression estimated associations between CF clinical characteristics, BALF inflammatory markers at two time points, and resistance in the patients with CF. Percent neutrophil and IL8 values differed between study sites (Pittman et al., 2017), hence study site is adjusted for all regression models. Type III F tests assessed whether the association between resistance and each clinical characteristic differed by site. The interaction was considered significant at an alpha <0.15 level. When statistically significant, estimated associations and standard errors are reported for each site, otherwise a single estimate is provided for the association. Analyses were conducted with SAS statistical analysis software, version 9.3 (SAS Institute Inc. SAS/IML 9.3 User's Guide. SAS Publishing, Cary, NC, USA; 2011.) and R environment for statistical Computing, version 3.6.1 (R Foundation for Statistical Computing, Vienna, Austria).

3. Results

18 infants with CF (11 females) and 7 control patients (1 female) were included. There was a difference in the number of females in the CF group versus the control group (p = 0.07). Median age at chest CT scan for infants with CF was 13 months (IQR: 12.9–15.2 months) compared to 15 months (IQR: 13.0–15.9) for controls. Other relevant characteristics were not different between the CF and control groups (Table 1, supplementary Table 1). The cohort of infants with CF from the USA were older than infants from Australia during the time of the chest CT scan, median age of 14.8 vs. 13.0 months (p = 0.03) (supplementary Table 1).

The same type of CT scanner (SIEMENS/SOMATOM Definition Flash) and kernel (I70f) were used for all scans in the Melbourne CF and control cohorts. The Melbourne CF scans were similar to each other in resolution (axial slice thickness 0.35 or 0.4 mm, axial pixel size range 0.348 to 0.434 mm), and the control scans were similar to each other (axial slice increment 0.7 mm, axial pixel size range 0.363 to 0.479 mm). Three of the 8 IU CF scans were obtained using a Philips/iCT SP scanner and YD kernel and the other 5 IU CF scans were obtained using a Philips/iCT 256 scanner and YC kernel. All IU scans had similar resolution to each other (axial slice thickness 1.0 mm, axial pixel size range 0.375 to 0.488 mm).

Models were created to approximately 5 generations (Fig. 3) with a median of 51 distal bronchi (interquartile range 46,56) used as outlets for flow in the CFD models (Table 2). The cross-sectional area of the models created from infants with CF appeared to be smaller at the tracheal inlet and the distal outlets, but not the main bronchi (Table 2) compared to controls.

Median airway resistance was higher and appears more variable in infants with CF vs. controls (0.09 [0.08, 0.14] vs. 0.07 [0.05, 0.09]) (p = 0.037) (Fig. 4). After trimming the models so that both groups had 33 outlets, the resistance remained increased in infants with CF (0.06 [0.05, 0.09] vs. 0.04 [0.04, 0.06) (p = 0.032) (Fig. 4). The difference was no longer statistically significant when the trimmed models were

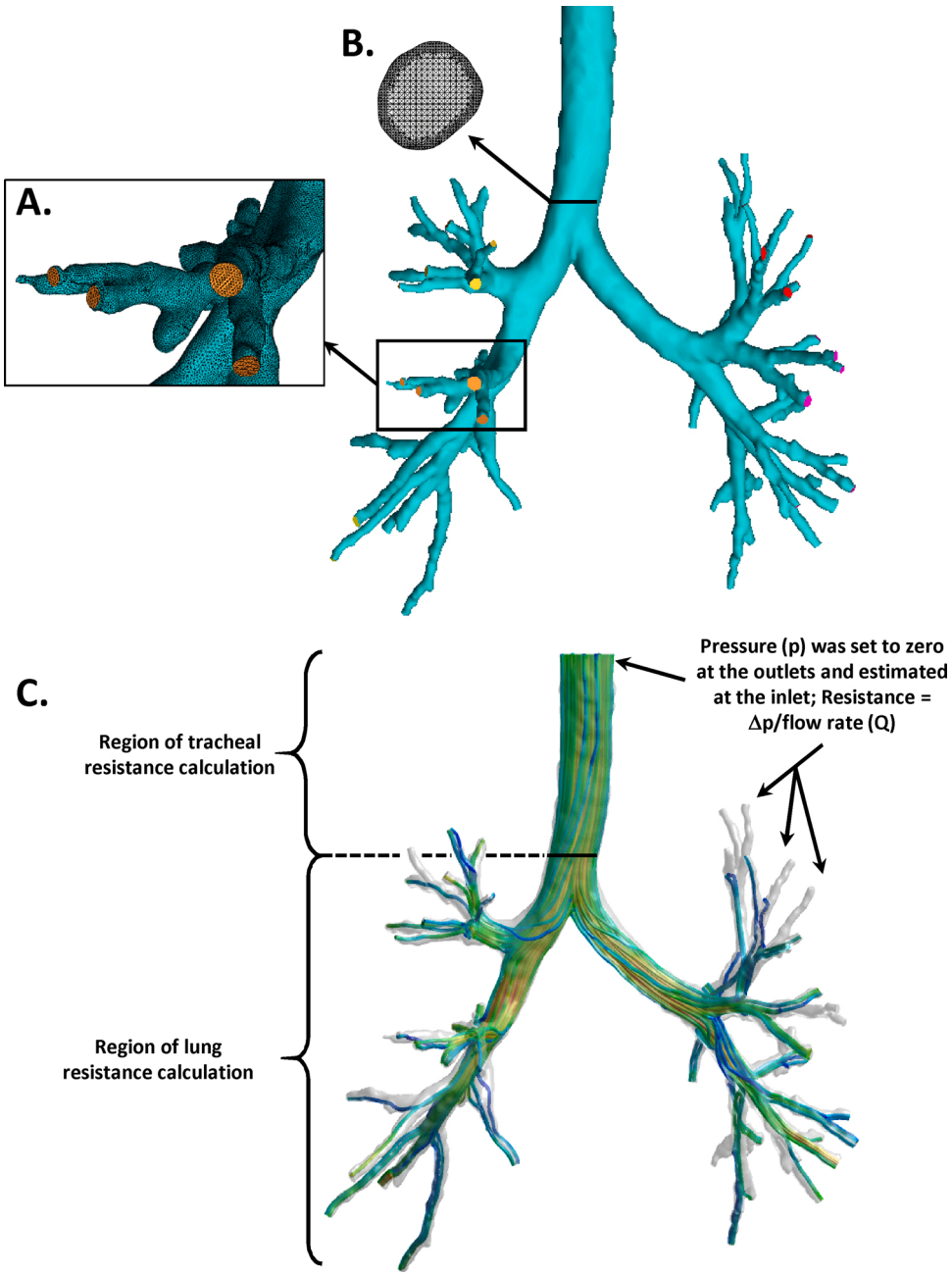

Fig. 2. Computational fluid dynamic model. (A) Detail showing distal airways trimmed cross-sectionally and the surface of the tetrahedral mesh. (B) Full airway geometry showing outlets clustered by lobe (indicated by color). Detail shows the tracheal plane with tetrahedral mesh. (C) Streamlines of inspiratory airflow estimated using computational fluid dynamics; red indicates faster velocities along streamlines, blue indicates slower velocities.

Table 1
Patient demographics at time of CT scan *Categorical variables presented as n (%) and continuous variables presented as median (interquartile range) ** Height and Weight available for 6/7 control infants.

	Control N = 7	CF N = 18
Age (mo)	15.0 [13.0, 15.93]	13.05 [12.9, 15.23]
Height (cm) **	80 [74.7, 84]	76.2 [74.5, 78]
Height for Age Z-score**	0.3 [-0.8, 1.59]	−0.02 [-0.55, 0.39]
Weight (kg)**	11.8 [9.1, 13.7]	10.28 [9.99, 10.7]
Weight for Age Z-score**	0.58 [-0.95, 1.9]	0.03 [-0.43, 0.32]
Weight for Height Z-score**	0.96 [0.43, 1.97]	0.29 [-0.16, 1.48]
Sex, F (N, (%))	1 (14.3)	11 (61.11)
F508del Homozygous (N, %))	N/a	11 (61.11)

scaled to the same inlet area (Fig. 4). Tracheal resistance and bronchial resistance tended to be higher in infants with CF in the full airway models, but the differences were not statistically different (Table 2).

Age, height, weight, weight for length Z score, and sex were not significantly associated with estimated resistance (Supplementary Table 2). As expected, smaller bronchial cross-sectional area measurements were associated with increased estimated airway resistance (Supplement Table 2).

Airway resistance was associated with increased percent neutrophils in the epithelial lining fluid at visit 1 (Table 3). The association differed between study sites at this visit (test for interaction <0.15), with $R^2 = 0.603$ ($p = 0.04$) for patients from Indianapolis and $R^2 = 0.563$ ($p = 0.012$) for patients from Melbourne. The association was not observed for Visit 2 (Fig. 5). Airway resistance was also associated with

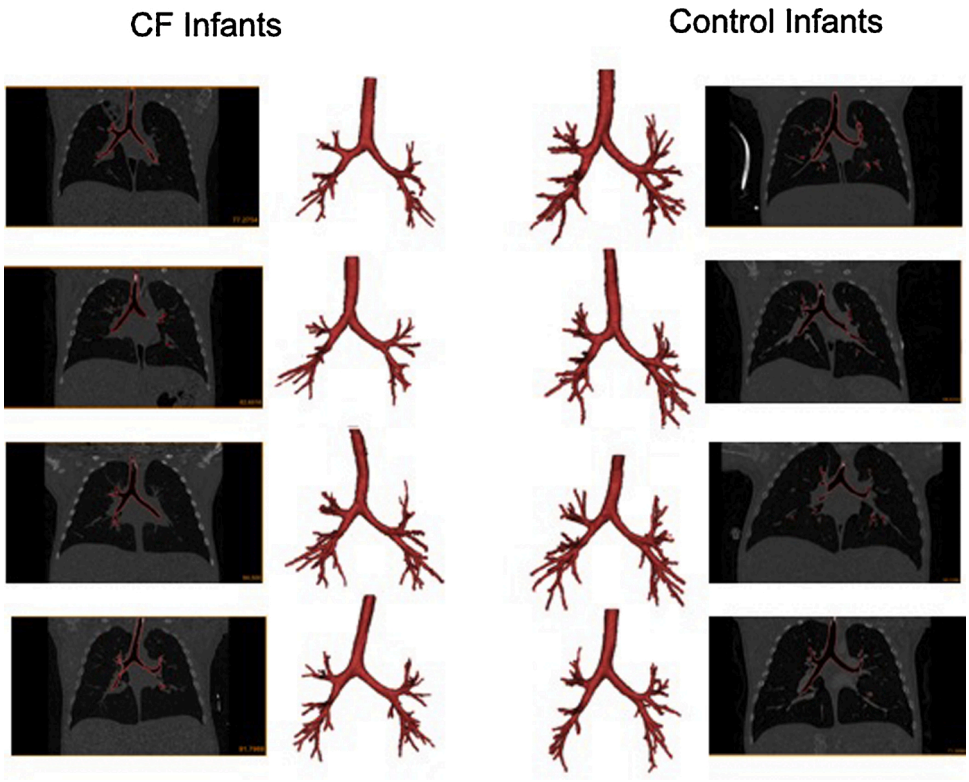

Fig. 3. Images of chest CT scans and airway segmentations from 4 CF infants and 4 control infants.

Table 2
Comparison of airway model measurements and CFD estimates between CF and control subjects. Median [IQR] and Exact Wilcoxon Rank Tests were conducted for the full airway models.

	Control N = 7	CF N = 18	p-value
FULL MODEL			
Tracheal Inlet Area (mm^2)	61.88 [54.53, 66.76]	52.32 [46.08, 60.87]	0.05
Right Main Bronchus Area (mm^2)	38.83 [35.5, 42.8]	35.11 [30.33, 40.46]	0.24
Left Main Bronchus Area (mm^2)	24.76 [19.92, 26.21]	22.06 [16.2, 23.62]	0.29
Right Outlets Area (mm^2)	48.48 [35.13, 53.19]	35.32 [29.78, 40.7]	0.03
Left Outlets Area (mm^2)	42.94 [31.59, 53.63]	30.76 [26.23, 36.43]	0.02
Outlet number	56 [48, 59]	50 [45, 54]	0.06
Airway resistance (Raw) (Pa/mL/sec)	0.07 [0.05, 0.09]	0.09 [0.08,0.14]	0.04
Tracheal resistance (Pa/mL/sec)	0.03 [0.01, 0.03]	0.03 [0.02,0.04]	0.18
Bronchial resistance (Pa/mL/sec)	0.04 [0.03, 0.06]	0.06 [0.05,0.09]	0.08

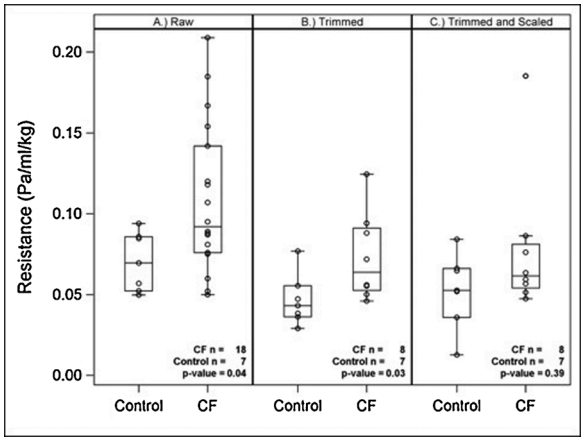

Fig. 4. Box plots of Resistance comparing the two groups (CF vs Control) using (A) Full airway models (Raw), (B) Trimmed models, and (C) Trimmed-and-scaled models.

an increase in log transformed IL8 measured in epithelial lining fluid from 8 months earlier (Visit 1) but the association was not seen in fluid collected at the same visit as the chest CT (Visit 2). Airway resistance was not associated with PRAGMA-CF CT scores for structural lung disease, or infant pulmonary function tests apart from an inverse association with FEF75 in the subjects from the USA at Visit 1 but not Visit 2 (Table 3). Only 12 infants had infant lung function data.

4. Discussion

CFD methodology translates airway anatomy into an estimate of pulmonary function, in this case airway resistance. If the airways are narrower, longer, or more tortuous, the resistance will increase. The models created from infants with CF do not appear visually abnormal (Fig. 3), but we found that estimates of airway resistance were higher in the infants with CF compared to controls. Tracheal resistance did not appear significantly different between the groups, indicating that the differentiating part of the airway may be in the distal branches of this model: the 5th to 6th generation bronchi. Because models created from control infant scans tended to have more outlets, some airway models were trimmed so that they had an equal number of outlets. After trimming, resistance remained increased in infants with CF. Scaling of the airway to eliminate size differences removed apparent differences in resistance between the two groups, implying that the smaller cross-sectional area of the model's distal airways is contributing to the difference. This smaller cross-sectional area may be innate or may be

Table 3
Results of univariate linear regression of CF clinical characteristics regressed on full model resistance. When the interaction is statistically significant, estimated associations and standard errors are reported for each study site, otherwise a single estimate is provided for the estimated association.

Clinical Measure	Estimate (SE)	Model R^2	p-value	n = Melbourne,IU (total)
% Neutrophils, Visit 1				10,7 (17)
IU	***0.11 (0.039)***	***0.603***	***0.04***	
Melbourne	***0.80 (0.25)***	***0.563***	***0.012***	
% Neutrophils, Visit 2	0.069 (0.065)	0.199	0.31	10,6 (16)
Log(Absolute Neutrophil Count), Visit 1	0.005 (0.003)	0.258	0.15	10,7 (17)
Log(Absolute Neutrophil Count), Visit 2	−0.001 (0.005)	0.13	0.83	10,6 (16)
Log(Interleukin 8), Visit 1	**0.021 (0.009)**	**0.38**	**0.04**	10,7 (17)
Log(Interleukin 8), Visit 2	0.015 (0.009)	0.27	0.13	10,7 (17)
PRAGMA-CF Bronchiectasis	−0.049 (0.063)	0.21	0.45	10,8 (20)
PRAGMA-CF % Airway Disease	0.144 (0.015)	0.23	0.34	10,8 (20)
FEV 0.5 Z-score, Visit 1	0.0006 (0.01)	0.12	0.96	4,8 (12)
FEV 0.5 Z-score, Visit 2	0.01 (0.03)	0.28	0.71	5,8 (13)
FEF 75 Z-score, Visit 1				4,8 (12)
IU	**-0.037 (0.014)**	**0.54**	**0.04**	
Melbourne	0.02 (0.02)	0.26	0.49	
FEF 75 Z-score, Visit 2				4,8 (12)
IU	0.022 (0.033)	0.07	0.53	
Melbourne	0.023 (0.028)	0.25	0.50	

related to early airway wall thickening decreasing the inner diameter of the airways. Airway inflammation measured by the percent neutrophils and IL8 in epithelial lining fluid at 4 months of age was correlated with airway resistance estimated on chest CT scans at 13 months, but inflammation at the time of CT imaging was not associated with airway resistance.

Like studies in the CF pig (Awadalla et al., 2014), estimated resistance appeared different between airways imaged from chest CTs of infants with CF compared to control infants imaged using the same protocol. Although the trachea inlets were smaller in CF, the trachea did not appear to drive the increased resistance. Outlet area was smaller in infants with CF versus controls, indicating that the most distal airways identified on the models appeared to have a smaller cross-sectional area (Table 2). In addition to normal airway tapering, this decrease may be due to poor airway distension (Meyerholz et al., 2018) or to thickened airway walls that further decrease lumen size of peripheral airways. In addition, the presence of airway wall thickening in CF makes airways more visible on chest CT (DeBoer et al., 2014) and may allow modeling to a greater length along individual branches. As the number of airway branches in the full models tended to be greater in the control infants than in infants with CF, poor airway distensibility may be more likely to explain the difference. Other studies have had variable conclusions on airway lumen size in CF (Humphries et al., 2015; Kuo et al., 2017; Mott et al., 2013). This could be due to differences in imaging or true changes in the CF airway over time, with airway wall thickening that may decrease lumen size initially, followed by progressive dilation and the development of bronchiectasis.

Inflammation and infection in the CF airway are associated with structural airway injury and development of bronchiectasis (Davis et al., 2007; DeBoer et al., 2014; Garratt et al., 2015; Sly et al., 2013). Sly and colleagues have shown that even in the youngest patients, neutrophil elastase in BALF is associated with later development of structural airway injury and bronchiectasis (Sly et al., 2013). Similarly, Brennan and colleagues have reported that neutrophils in BALF is associated with worsening airway mechanics based on increases in bronchial resistance measured by forced oscillation in infants with CF (Brennan et al., 2005). In our international cohort with varying levels of inflammation, percent

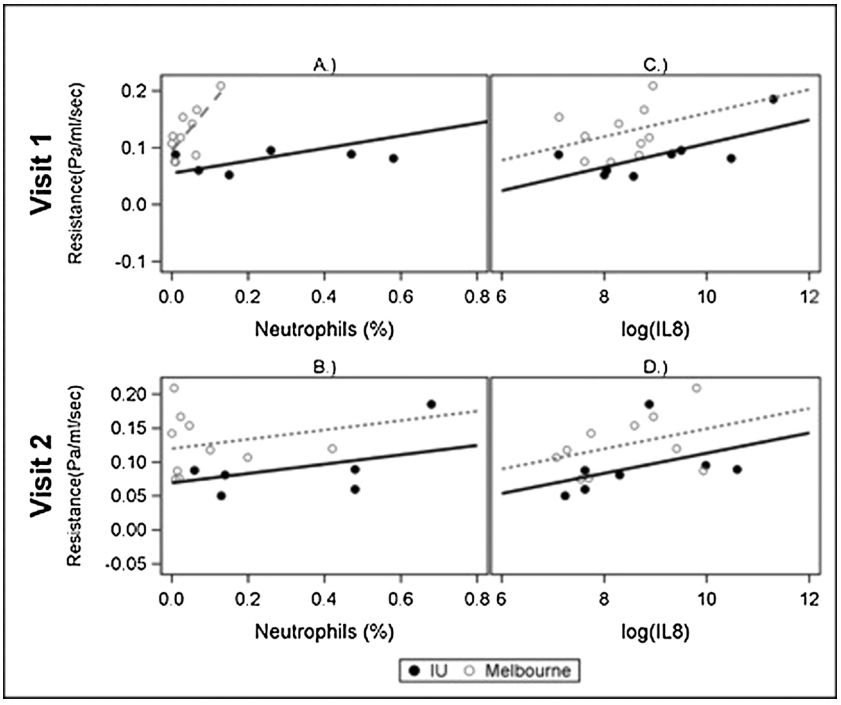

Fig. 5. Correlation of % Neutrophils and Log Interleukin 8 (IL8) from epithelial lining fluid with Resistance (in CF Subjects only) at Visit 1 and Visit 2. Non-parallel slopes (A) indicate a significant study site interaction p-value (<0.15). Parallel slopes (B,C,D) indicate that the interaction p-value was not significant (>0.15).

neutrophils and IL-8, measured in BALF at the median age of 4 months, were associated with increased estimates of airway resistance at the median age of 13 months. Based on this association with early inflammation and lack of significant cross-sectional association with inflammatory markers, we hypothesize that early airway inflammation contributed to airway wall thickening and the small cross-section of distal airways and increased airway resistance in the medium sized 5th and 6th generation airways and smaller. In CF, bronchiectasis often develops in the upper lobes first, but BALF is commonly obtained from the right middle lobe and lingula. This anatomic discrepancy may have limited the cross-sectional association in this cohort. Further evaluation of airway remodeling by generation in young children is needed to validate this hypothesis.

PRAGMA-CF scores measure visible evidence of structural airway injury from chest CT scans (Rosenow et al., 2015). PRAGMA-CF bronchiectasis and airway wall thickening scores were not associated with the changes in estimated airway resistance in this cohort. Our CFD modeling is estimating the effects of the central airway lumen size rather than this distal structural injury. It is unclear if the inflammation affects central and distal airways in the same pattern. Infant PFTs have been reported to be abnormal in infants with CF and associated with exacerbations and other important longitudinal outcomes (Brumback et al., 2013; Davis et al., 2010; Pittman et al., 2012; Ranganathan et al., 2008). PFTs give a composite outcome similar to estimated CFD resistance, however CFD simulations also allow estimation of flow by lobe, regional ventilation, airflow patterns, and particle deposition. With further study, CFD could be used to more deeply explore the impact of these airway abnormalities.

Limitations include the small sample size, which may contribute to type II error in our secondary outcomes. The small sample size also limits our ability to perform multivariate analysis and adjust for sex and patient size and the disproportion of females in the control cohort may contribute to larger airway size (Liptzin et al., 2015). The CT scans were obtained for PRAGMA-CF scoring and not specifically for the CFD analysis; therefore, the endotracheal tubes in the trachea prevent full evaluation of tracheal and glottic differences, which has been seen in the CF pig (Awadalla et al., 2014). In addition, our CFD methodology analyzes flow through a static model at full inspiration. The CFD model based on steady state inspiratory airflow measured from our control cohort does not simulate breathing with flow driven by the negative intrathoracic pressure, rather it is a summative model of the effects of airway size and shape on airflow resistance. For simplicity, our method did not model distensibility of airways or regional compliance, and it is not clear if the CF and control airways have different distensibility. The lobar volume changes based on volumetric inspiratory and expiratory scans help to reassure that the simulated flow distribution was approximately physiologic (Supplement Fig. 1). In addition, although the association between % neutrophils and resistance was consistent across continents, the baseline difference in inflammation between the infants from Australia and those from the USA presents some limitation to the interpretation of results (Pittman et al., 2017).

Segmentation of the airways relied on dynamic region growing which uses both pixel gray value (density) and proximity to find pixels surrounding a selected pixel within a specified range. Pixel density and proximity could be affected by CT resolution and kernel sharpness. However, the lower resolution and potential difference in sharpness of the IU CT scans compared to those of the Melbourne CF cohort (slice thickness 1.0 mm (IU) vs. 0.35−0.4 mm (Melbourne CF); kernel YC or YD (IU) vs. I70f\3 (Melbourne CF)) did not appear to affect the number of outlets either in average total (49.3 (IU) vs. 48.6 (Melbourne), $p > 0.8$) or in average number per lobe (minimum $p > 0.08$). In addition, identical segmentation parameters produced different numbers of outlets within cohorts with the same CT quality, suggesting real physiological differences between children.

Estimates of lung function are useful for outcomes in clinical trials, to assess personalized response to drugs, and for long-term monitoring. Ideally results would be compared to robust lung function measurements, but lung function measurements were limited in this cohort. The need for sedation to conduct infant PFTs has limited widespread clinical use. Although the CFD methodology is complicated, chest CT imaging, and potentially MRI imaging in the future, is a widespread and useful diagnostic modality that could be adapted for not only structural but also functional assessment of early CF lung disease.

In conclusion, we created airway models from inspiratory chest CT images and performed CFD estimates of resistance that were elevated in infants with CF compared to controls. These results also support that airway inflammation and structural airway changes, as assessed through CFD estimates of resistance, are related; studies aiming to mitigate inflammation to prevent future lung injury in preschool children with CF are indicated. Computational fluid dynamic methods can add value to imaging data as a measure of early airway dysfunction or potentially, may be used to assess response to interventions.

Author contributions

Emily M DeBoer: Investigation, Writing Original draft, Review, and Editing

Julia S Kimbell: Conceptualization, Methodology, Validation, Investigation

Kaci Pickett: Formal analysis, Writing – Review and Editing

Joseph E Hatch: Investigation, resources, project administration, Writing Review and Editing

Kathryn Akers: Resources, Investigation

John Brinton: Formal analysis

Graham L Hall: Conceptualization, Editing

Louise King: Resources, project administration

Fiona Ramanauskas: Investigation

Tim Rosenow: Resources, Investigation

Stephen M Stick: Conceptualization, Investigation

Harm A Tiddens: Conceptualization, Investigation

Thomas W Ferkol: Conceptualization, Supervision, Funding acquisition

Sarath C Ranganathan: Conceptualization, Supervision, Funding acquisition

Stephanie D Davis: Conceptualization, Supervision, Funding acquisition, Writing – Review and Editing

Funding

Supported by NHLBI Viral Pathogenesis of Early CF Lung Disease study (R01HL116211) PI Davis, Ferkol, Ranganathan, DeBoer 18A0 Cystic Fibrosis Foundation, and AREST CF NHMRC1043768 PI Ranganathan, and NIH/NCATS Colorado CTSI UL1 TR002535. Contents are the authors' sole responsibility and do not necessarily represent official NIH views.

Declaration of Competing Interest

Dr. DeBoer reports grants from Cystic Fibrosis Foundation, grants from NIH/NCATS Colorado CTSI, during the conduct of the study; personal fees from Boehringer Ingelheim, personal fees from Triple Endoscopy, outside the submitted work. In addition, Dr. DeBoer has a patent Endoscopic methods and technologies pending. Dr. Kimbell reports grants from Indiana University, during the conduct of the study; grants from Applied Research Associates, Inc., grants from Kitware, Inc., outside the submitted work;. Dr. Rosenow has a patent PCT/AU2016/000079 issued. Dr. Tiddens is heading the Erasmus MC core laboratory Lung Analysis which is a not-for-profit core image analysis laboratory. The financial aspects of the laboratory are handled by the department of Radiology and by the Sophia Research BV. FLUIDDA has developed computational fluid dynamic modelling based on chest-CTs obtained from Erasmus MC-Sophia for which royalties are received by Sophia

Research BV. Dr. Ferkol reports several grants from NIH during the conduct of the study; and support from Parion Sciences and Aerocrine Pharmaceuticals (Circassia) for clinical and device trials unrelated to the work presented in this manuscript. Dr. Davis reports grants from NHLBI, grants from Cystic Fibrosis Foundation, during the conduct of the study. Outside the submitted work, she was a reviewer of grants for Vertex Pharmaceuticals and is currently an editor for a book on cystic fibrosis for Springer. The other authors have nothing to disclose.

Acknowledgements

The authors thank Nadeene Clarke, Royal Children's Hospital Melbourne, for her quick response to questions. The authors thank Dr. Rob Tepper for his stimulating conversation about airways. Dr. DeBoer thanks Drs. Scott Sagel, Robin Deterding, Bradford Smith, and Deb Liptzin for their support and mentorship in this project.

Appendix A. Supplementary data

Supplementary material related to this article can be found, in the online version, at doi:https://doi.org/10.1016/j.resp.2021.103722.

References

Awadalla, M., Miyawaki, S., Abou Alaiwa, M.H., Adam, R.J., Bouzek, D.C., Michalski, A. S., Fuld, M.K., Reynolds, K.J., Hoffman, E.A., Lin, C.L., Stoltz, D.A., 2014. Early airway structural changes in cystic fibrosis pigs as a determinant of particle distribution and deposition. Ann. Biomed. Eng. 42, 915–927.

Ben-Dov, G., Cohen, J., 2007. Critical Reynolds number for a natural transition to turbulence in pipe flows. Phys. Rev. Lett. 98, 064503.

Bos, A.C., van Holsbeke, C., de Backer, J.W., van Westreenen, M., Janssens, H.M., Vos, W. G., Tiddens, H.A., 2015. Patient-specific modeling of regional antibiotic concentration levels in airways of patients with cystic fibrosis: are we dosing high enough? PLoS One 10, e0118454.

Brennan, S., Hall, G.L., Horak, F., Moeller, A., Pitrez, P.M., Franzmann, A., Turner, S., de Klerk, N., Franklin, P., Winfield, K.R., Balding, E., Stick, S.M., Sly, P.D., 2005. Correlation of forced oscillation technique in preschool children with cystic fibrosis with pulmonary inflammation. Thorax 60, 159–163.

Brumback, L.C., Davis, S.D., Kerby, G.S., Kloster, M., Johnson, R., Castile, R., Hiatt, P.W., Hart, M., Rosenfeld, M., 2013. Lung function from infancy to preschool in a cohort of children with cystic fibrosis. Eur. Respir. J. 41, 60–66.

Davis, S.D., Fordham, L.A., Brody, A.S., Noah, T.L., Retsch-Bogart, G.Z., Qaqish, B.F., Yankaskas, B.C., Johnson, R.C., Leigh, M.W., 2007. Computed tomography reflects lower airway inflammation and tracks changes in early cystic fibrosis. Am. J. Respir. Crit. Care Med. 175, 943–950.

Davis, S.D., Rosenfeld, M., Kerby, G.S., Brumback, L., Kloster, M.H., Acton, J.D., Colin, A. A., Conrad, C.K., Hart, M.A., Hiatt, P.W., Mogayzel, P.J., Johnson, R.C., Wilcox, S.L., Castile, R.G., 2010. Multicenter evaluation of infant lung function tests as cystic fibrosis clinical trial endpoints. Am. J. Respir. Crit. Care Med. 182, 1387–1397.

DeBoer, E.M., Swiercz, W., Heltshe, S.L., Anthony, M.M., Szefler, P., Klein, R., Strain, J., Brody, A.S., Sagel, S.D., 2014. Automated CT scan scores of bronchiectasis and air trapping in cystic fibrosis. Chest 145, 593–603.

Deschamp, A.R., Hatch, J.E., Slaven, J.E., Gebregziabher, N., Storch, G., Hall, G.L., Stick, S., Ranganathan, S., Ferkol, T.W., Davis, S.D., 2019. Early respiratory viral infections in infants with cystic fibrosis. J. Cyst. Fibros. 18, 844–850.

Fischer, A.J., Singh, S.B., Adam, R.J., Stoltz, D.A., Baranano, C.F., Kao, S., Weinberger, M.M., McCray Jr, P.B., Starner, T.D., 2014. Tracheomalacia is associated with lower FEV1 and Pseudomonas acquisition in children with CF. Pediatr. Pulmonol. 49, 960–970.

Frank-Ito, D.O., Kimbell, J.S., Borojeni, A.A.T., Garcia, G.J.M., Rhee, J.S., 2019. A hierarchical stepwise approach to evaluate nasal patency after virtual surgery for nasal airway obstruction. Clin, Biomech, (Bristol, Avon) 61, 172–180.

Garratt, L.W., Sutanto, E.N., Ling, K.M., Looi, K., Iosifidis, T., Martinovich, K.M., Shaw, N.C., Kicic-Starcevich, E., Knight, D.A., Ranganathan, S., Stick, S.M., Kicic, A., Australian Respiratory Early Surveillance Team for Cystic, F, 2015. Matrix metalloproteinase activation by free neutrophil elastase contributes to bronchiectasis progression in early cystic fibrosis. Eur. Respir. J. 46, 384–394.

Gunatilaka, C.C., Higano, N.S., Hysinger, E.B., Gandhi, D.B., Fleck, R.J., Hahn, A.D., Fain, S.B., Woods, J.C., Bates, A.J., 2020. Increased Work of Breathing due to Tracheomalacia in Neonates. Ann. Am. Thorac. Soc. 17, 1247–1256.

Ho, C.Y., Liao, H.M., Tu, C.Y., Huang, C.Y., Shih, C.M., Su, M.Y., Chen, J.H., Shih, T.C., 2012. Numerical analysis of airflow alteration in central airways following tracheobronchial stent placement. Exp. Hematol. Oncol. 1, 23.

Hof, B., Juel, A., Mullin, T., 2003. Scaling of the turbulence transition threshold in a pipe. Phys. Rev. Lett. 91, 244502.

Humphries, S.M., Hunter, K.S., Shandas, R., Deterding, R.R., DeBoer, E.M., 2015. Analysis of pediatric airway morphology using statistical shape modeling. Med. Biol. Eng. Comput.

Kimbell, J.S., Subramaniam, R.P., Gross, E.A., Schlosser, P.M., Morgan, K.T., 2001. Dosimetry modeling of inhaled formaldehyde: comparisons of local flux predictions in the rat, monkey, and human nasal passages. Toxicol. Sci. 64, 100–110.

Kimbell, J.S., Frank, D.O., Laud, P., Garcia, G.J., Rhee, J.S., 2013. Changes in nasal airflow and heat transfer correlate with symptom improvement after surgery for nasal obstruction. J. Biomech. 46, 2634–2643.

Kuo, W., Soffers, T., Andrinopoulou, E.R., Rosenow, T., Ranganathan, S., Turkovic, L., Stick, S.M., Tiddens, H., Arest, C.F., 2017. Quantitative assessment of airway dimensions in young children with cystic fibrosis lung disease using chest computed tomography. Pediatr. Pulmonol. 52, 1414–1423.

Liptzin, D.R., Landau, L.I., Taussig, L.M., 2015. Sex and the lung: observations, hypotheses, and future directions. Pediatr. Pulmonol. 50, 1159–1169.

Meyerholz, D.K., Stoltz, D.A., Namati, E., Ramachandran, S., Pezzulo, A.A., Smith, A.R., Rector, M.V., Suter, M.J., Kao, S., McLennan, G., Tearney, G.J., Zabner, J., McCray Jr, P.B., Welsh, M.J., 2010. Loss of cystic fibrosis transmembrane conductance regulator function produces abnormalities in tracheal development in neonatal pigs and young children. Am. J. Respir. Crit. Care Med. 182, 1251–1261.

Meyerholz, D.K., Stoltz, D.A., Gansemer, N.D., Ernst, S.E., Cook, D.P., Strub, M.D., LeClair, E.N., Barker, C.K., Adam, R.J., Leidinger, M.R., Gibson-Corley, K.N., Karp, P. H., Welsh, M.J., McCray Jr, P.B., 2018. Lack of cystic fibrosis transmembrane conductance regulator disrupts fetal airway development in pigs. Lab. Invest. 98, 825–838.

Mott, L.S., Graniel, K.G., Park, J., de Klerk, N.H., Sly, P.D., Murray, C.P., Tiddens, H.A., Stephen, M.S., Arest, C.F., 2013. Assessment of early bronchiectasis in young children with cystic fibrosis is dependent on lung volume. Chest 144, 1193–1198.

Nguyen, T.T., Hoo, A.F., Lum, S., Wade, A., Thia, L.P., Stocks, J., 2013. New reference equations to improve interpretation of infant lung function. Pediatr. Pulmonol. 48, 370–380.

O'Sullivan, B.P., Freedman, S.D., 2009. Cystic fibrosis. Lancet 373, 1891–1904.

Pittman, J.E., Johnson, R.C., Davis, S.D., 2012. Improvement in pulmonary function following antibiotics in infants with cystic fibrosis. Pediatr. Pulmonol. 47, 441–446.

Pittman, J.E., Wylie, K.M., Akers, K., Storch, G.A., Hatch, J., Quante, J., Frayman, K.B., Clarke, N., Davis, M., Stick, S.M., Hall, G.L., Montgomery, G., Ranganathan, S., Davis, S.D., Ferkol, T.W., Australian Respiratory Early Surveillance Team for Cystic, F, 2017. Association of antibiotics, airway microbiome, and inflammation in infants with cystic fibrosis. Ann. Am. Thorac. Soc. 14, 1548–1555.

Qi, S., Li, Z., Yue, Y., van Triest, H.J., Kang, Y., 2014. Computational fluid dynamics simulation of airflow in the trachea and main bronchi for the subjects with left pulmonary artery sling. Biomed. Eng. Online 13, 85.

Ramsey, K.A., Rosenow, T., Turkovic, L., Skoric, B., Banton, G., Adams, A.M., Simpson, S. J., Murray, C., Ranganathan, S.C., Stick, S.M., Hall, G.L., Arest, C.F., 2016. Lung clearance index and structural lung disease on computed tomography in early cystic fibrosis. Am. J. Respir. Crit. Care Med. 193, 60–67.

Ranganathan, S., Linnane, B., Nolan, G., Gangell, C., Hall, G., 2008. Early detection of lung disease in children with cystic fibrosis using lung function. Paediatr. Respir. Rev. 9, 160–167.

Ranganathan, S.C., Hall, G.L., Sly, P.D., Stick, S.M., Douglas, T.A., Australian Respiratory Early Surveillance Team for Cystic, F, 2017. Early lung disease in infants and preschool children with cystic fibrosis. What have we learned and what should we do about it? Am. J. Respir. Crit. Care Med. 195, 1567–1575.

Rennard, S.I., Basset, G., Lecossier, D., O'Donnell, K.M., Pinkston, P., Martin, P.G., Crystal, R.G., 1986. Estimation of volume of epithelial lining fluid recovered by lavage using urea as marker of dilution. J. Appl. Physiol. 1985 (60), 532–538.

Reynisson, P.J., Scali, M., Smistad, E., Hofstad, E.F., Leira, H.O., Lindseth, F., Nagelhus Hernes, T.A., Amundsen, T., Sorger, H., Lango, T., 2015. Airway segmentation and centerline extraction from thoracic CT - comparison of a new method to state of the art commercialized methods. PLoS One 10, e0144282.

Rosenow, T., Oudraad, M.C., Murray, C.P., Turkovic, L., Kuo, W., de Bruijne, M., Ranganathan, S.C., Tiddens, H.A., Stick, S.M., Australian Respiratory Early Surveillance Team for Cystic, F, 2015. PRAGMA-CF. A quantitative structural lung disease computed tomography outcome in Young Children with cystic fibrosis. Am. J. Respir. Crit. Care Med. 191, 1158–1165.

Sanders, D.B., Li, Z., Laxova, A., Rock, M.J., Levy, H., Collins, J., Ferec, C., Farrell, P.M., 2014. Risk factors for the progression of cystic fibrosis lung disease throughout childhood. Ann. Am. Thorac. Soc. 11, 63–72.

Simpson, S.J., Mott, L.S., Esther Jr, C.R., Stick, S.M., Hall, G.L., 2013. Novel end points for clinical trials in young children with cystic fibrosis. Expert Rev. Respir. Med. 7, 231–243.

Sly, P.D., Gangell, C.L., Chen, L., Ware, R.S., Ranganathan, S., Mott, L.S., Murray, C.P., Stick, S.M., Investigators, A.C., 2013. Risk factors for bronchiectasis in children with cystic fibrosis. N. Engl. J. Med. 368, 1963–1970.

Wofford, M.R., Kimbell, J.S., Frank-Ito, D.O., Dhandha, V., McKinney, K.A., Fleischman, G.M., Ebert Jr, C.S., Zanation, A.M., Senior, B.A., 2015. A computational study of functional endoscopic sinus surgery and maxillary sinus drug delivery. Rhinology 53, 41–48.